

# UC Berkeley

## UC Berkeley Previously Published Works

### Title

Objective Quantification of Fluorescence Intensity on the Corneal Surface Using a Modified Slit-lamp Technique

### Permalink

<https://escholarship.org/uc/item/2wz41636>

### Journal

Eye & Contact Lens Science & Clinical Practice, 39(3)

### ISSN

1542-2321

### Authors

Tan, Bo  
Zhou, Yixiu  
Svitova, Tatyana  
et al.

### Publication Date

2013-05-01

### DOI

10.1097/icl.0b013e31828dc7f3

Peer reviewed

# Objective Quantification of Fluorescence Intensity on the Corneal Surface Using a Modified Slit-lamp Technique

*Bo Tan, Ph.D., Yixiu Zhou, Ph.D., Tatyana Svitova, Ph.D., and Meng C. Lin, O.D., Ph.D.*

**Objectives:** To improve the digital quantification of fluorescence intensity of sodium fluorescein instilled on corneal surface by modifying a slit lamp hardware and performing computerized processing of captured digital images.

**Methods:** The optics of a slit lamp were modified to remove corneal Purkinje reflection and to expand the illuminated area on the cornea, followed by postexperiment image processing to minimize the influence of uneven illumination. To demonstrate the feasibility and reliability of this new technique, we applied it to objective grading of corneal staining with sodium fluorescein. The results of computerized grading were compared with the results obtained using standard subjective grading of corneal staining. Objective digital grades, staining area, and staining pixel with manually and automatically defined threshold (SP-M and SP-A) were calculated for both original and processed images. Standard subjective grades of the original images were performed by 13 trained observers using National Eye Institute (NEI), Efron, and CCLRU grading scales. A series of linear regression analyses were performed to investigate the correlation between objective and subjective grades.

**Results:** Digital grades of the captured images were correlated significantly with subjective grades. After minimization of the artifact caused by the nonuniform illumination, correlations between digital and subjective grading were mostly strengthened. In some cases, digital grading of corneal staining was more sensitive than subjective grading methods when differentiating subtle differences of corneal staining.

**Conclusions:** Modifications performed on commercial slit-lamp hardware and the proposed digital image-processing technique have improved the quality of captured images for semiautomated quantification of fluorescein intensity on the cornea.

**Key Words:** Fluorescence—Corneal staining—Image processing—Fluorescein quenching.

*(Eye & Contact Lens 2013;39: 239–246)*

From the Clinical Research Center, School of Optometry, University of California, Berkeley, CA.

Supported in part by the University of California at Berkeley Clinical Research Center with unrestricted funds from Carl Zeiss Vision, Cooper Vision, Roberta J. Smith research fund, and the Morton Sarver Foundation.

The original poster “Improving Objective Grading of Corneal Staining by Eliminating the Influence of Corneal Reflection and the Uneven Distribution of Fluorescence Excitation” was presented at the American Academy of Optometry Annual Meeting, in Boston, on October 14th, 2011.

The authors have no other funding or conflicts of interest to disclose.

Address correspondence and reprint requests to Meng C. Lin, O.D., Ph.D., Clinical Research Center, School of Optometry, University of California, Berkeley, 360 Minor Hall, Berkeley, CA 94720-2020; e-mail: mlin@berkeley.edu

Accepted February 17, 2013.

DOI: 10.1097/ICL.0b013e31828dc7f3

Fluorescent dyes have been commonly used as tracers for many clinical applications. Sodium fluorescein, in particular, has been broadly used to evaluate ocular surface integrity. In addition to sodium fluorescein dye, other derivatives with larger molecular weights (e.g., fluorescein isothiocyanate and Fluorosoft) have also been useful in examining precorneal and pre- and post-contact lens tear film, as well as evaluating contact lens fitting. Therefore, it is essential to objectively analyze fluorescence images in a quantitative manner.

It is not a trivial task to quantify the fluorescence intensity on the ocular surface because it is affected by several factors, including but not limited to concentration and thickness of fluorescein solution,<sup>1</sup> both of which are influenced by tear volume, tear film thickness, tear mixing, and tear turnover rate. An objective quantification of fluorescence intensity in the eye requires fluorometry. However, in clinical practice, it can be achieved alternatively by computer-aided image analysis of green color, which has been shown to attain superior inter- and intraobserver repeatability, compared with subjective quantification made by clinicians.<sup>2</sup> To perform objective image analysis, a high-quality fluorescence image of anterior ocular surface recorded by slit-lamp imaging system is one of the prerequisites. Nevertheless, most commercially available slit lamps have limitations in providing fluorescence images with the quality suitable for objective quantifications. Figure 1 shows a typical corneal fluorescence image taken by a conventional slit lamp, Nikon FS-2 (Nikon Corporation, Ophthalmic Instruments Section, Tokyo, Japan). There is a bright corneal Purkinje reflection or “hot spot” formed by the excitation light that is reflected off the cornea and then travels through the imaging path of the slit lamp. With this slit lamp, it is also difficult to illuminate uniformly the entire cornea without a diffuser when the cornea is in focus, especially for an eye with a large corneal diameter. Furthermore, given the optics of a slit lamp and curvatures of the human cornea, it is reasonable to assume that the illuminated light cannot be evenly distributed without modification of the current setup. Uneven illumination may obscure subtle characteristics of the corneal surface highlighted by fluorescein dyes or introduce optical artifacts.

Another aspect to consider in capturing good quality images is the concentration and volume of instilled sodium fluorescein solutions. Because the amount of fluorescein dye instilled onto the eye is commonly not quantitatively controlled in clinical practice, the initial concentration of fluorescein dye solution on the ocular surface on instillation could vary by an unknown magnitude. Thus, quenching can occur in some cases. It is therefore imperative to control initial fluorescein concentration and volume instilled onto eyes to avoid quenching and to help capture an image with a fluorescein concentration corresponding to optimal fluorescence

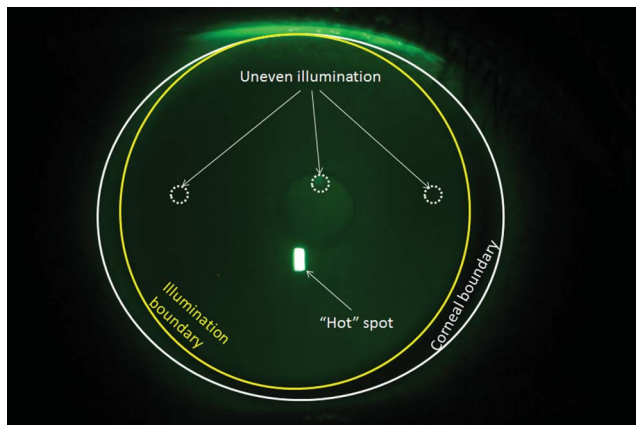


FIG. 1. Limitation of current imaging technique for corneal staining: hot spot; nonuniform and small illumination area.

intensity within the region where fluorescence intensity is linear with its concentration.

In this study, we present a method for hardware modification to a commercial slit lamp and a postexperiment image-processing technique as well as recommending an optimal sodium fluorescein concentration all aimed to capture high-quality ocular surface images for semiautomated quantification of fluorescein intensity.

## MATERIALS AND METHODS

### Modification of Hardware and Image-Processing Technique

A Nikon FS-2 slit lamp was modified by replacing its standard Nikon 35-mm film camera with a digital Canon EOS 7D camera (Canon, Inc., Tokyo, Japan). This digital camera allows an operator to release the shutter without having a lens attached. A ring adapter, Novoflex Lens Mount Adapter—Nikon Lens to Canon EOS Body (NOVOFLEX, Memmingen, Germany)—was used to mount the camera onto the original Nikon-designed mount on the slit lamp. We then followed the instructions provided by the previously published technical report<sup>3</sup> to make the modification, including mounting the camera body and synchronizing the shutter release with an external flash.

Removal of the “hot spot” in corneal fluorescence images has been demonstrated by Cox and Fonn.<sup>4</sup> However, the excitation filter used in their work was not readily available. In this study, we used an advanced filter set with similar cutoff wavelength and higher overall transmission efficiency: band-pass filter “ET470/40X” (wavelength, 470 nm; bandwidth [full width at half maximum], 40 nm) and long-pass filter “HQ510LP” (wavelength, 510 nm; band pass, >510 nm) (Chroma Technology Corp, Bellows Falls, VT). In Appendix 1, we have explained the necessity of this modification. The observation with the slit lamp should certainly be conducted in a dark room so that no stray light entered the optical system. Therefore, only the illumination from the slit-lamp light tower could pass through the excitation filter, reach the cornea, and excite the fluorescein dye. After replacing the filters, we also expanded the illumination area by enlarging the working distance (WD) between the cornea and the light source of the slit lamp, as shown in Appendix 1.

Although an improved corneal fluorescence image was obtained after the modifications mentioned above, uneven illumination on the cornea was still a challenge. The artificial patterns from uneven illumination could potentially mislead clinicians. Some clinicians, if noticing the patterns, would rotate the illumination tower of the slit lamp to try different incident angles of illumination. But if the patterns were neglected, a misjudgment of the fluorescence intensity on the cornea might occur. We then developed a method of postexperiment image processing to convert the original image into an image taken at quasi-even illumination. The image processing was summarized by a mathematical model as shown in equation 1. The validation of this equation is explained in Appendix 2.

$$\text{True fluorescence intensity} = \frac{\text{Original fluorescence intensity of each pixel}}{\text{Weight of each pixel}} \quad (1)$$

### Subjects

Subjects between 18 and 36 years old (18 women and 4 men) with an ocular surface disease index score of less than 13 were recruited through campus fliers and direct referrals. Informed consent was obtained from all study participants after a full description of the goals, potential risks and benefits, and procedures of the studies. This research project adhered to the tenets of the Declaration of Helsinki; it was approved by an institutional review board (Committee for Protection of Human Subjects, University of California, Berkeley, CA) and was HIPAA-compliant.

### Determination of the Concentration and Volume of Sodium Fluorescein

To capture the optimal fluorescence image, we should find a fluorescein concentration yielding optimal fluorescence intensity. An experiment was conducted using a tear film model formed by a thin film of sodium fluorescein solution “sandwiched” by two coverslips. We captured the fluorescence images of the tear film model at 12 different concentration levels (between 0.01% and 2%) and then measured the average pixel intensity in the image using image analysis software, Vision Assistant 2010, NI LabVIEW Vision Development Module (LabView; National Instruments, Austin, TX). The experiment results are shown in Appendix 3.

### Protocol

The procedure for imaging corneal staining in this study is as follows:

1. Instill sodium fluorescein solution (2% Fluorescein Ophthalmic Solution was purchased from Leiter’s Pharmacy, San Jose, CA) with a pipette onto the conjunctiva of the subject’s right eye and instruct the subject to close the eye and roll the eyeball to distribute the fluorescein dye evenly.
2. Ask the subject to put his/her chin on pre-cleaned chin rest and avoid moving.
3. Align the slit lamp, focus the camera on the subject’s right cornea, and snap the first image immediately after asking the subject to blink (to minimize the artifact caused by tear film break-up or local quenching effect).
4. Take the images with an interval of 30 sec until fluorescence intensity appeared to drop. In doing so, we were able to capture the optimal fluorescence intensity.

5. Repeat steps 1 to 4 for the subject’s left eye.
6. Image a white diffusive surface with the same setting of the illumination to obtain the intensity distribution of the excitation light so that postexperiment processing could be performed on the images.

### Data Analysis

To objectively grade the digital image of corneal staining and investigate the correlation between objective grading and subjective grading system, we first defined the criteria for quantification of the corneal staining severity. We used two factors: staining area (SA) and staining pixels (SP). Staining area was defined as the ratio of the pixel number of the corneal SA, defined by a freehand shape, to the total pixel number in the area of interest (equation 2). Staining pixel was the ratio of the pixel number of corneal staining, defined by the thresholding method, to the total number of pixels in the area of interest (equation 3). The software for image processing (including the image processing based on equation 1 to create a quasi-even illumination) was Vision Assistant 2010, NI LabVIEW Vision Development Module.

$$SA = \frac{\text{Number of pixel in the bounded staining area}}{\text{Number of pixel in the whole area of interest}} \times 100\%, \tag{2}$$

$$SP = \frac{\text{Number of staining pixel}}{\text{Number of pixel in the whole area of interest}} \times 100\%. \tag{3}$$

To calculate SA, one observer needed to visually inspect the image and use a freehand tool provided by Vision Assistant to define a region containing all the staining points. The pixels within the bounded region could be counted by the software and then the SA was calculated.

To calculate SP, we assigned a threshold value of the intensity so that the staining pixels could stand out and be counted. Two

techniques were applied to define the threshold value. One was to define the threshold value manually by inspecting each image and adjusting the threshold value until most SPs in the image stood out. The other was to assign a threshold value in a more “automatic” and statistical way. The calculation of this automatic threshold value was based on the statistics of the ratios of the “manual” threshold value and the maximum intensity of each image. We first selected the appropriate threshold value for each image manually and then calculated the individual ratio of each threshold value to the highest intensity of that image. The average of all the ratios from all the images was calculated as a generalized ratio. Then, the “automatic” threshold value for each image could be obtained by multiplying the generalized ratio to that image’s maximum intensity. Once the threshold, obtained from either manual or automatic method, was assigned to the image, SP could be counted by the software. Therefore, we obtained two SP values—manually defined threshold (SP-M) and automatically defined threshold (SP-A) for each image.

### Comparison Between Subjective and Objective Grading Systems

To validate the objective grades, SA, SP-M, and SP-A, we investigated the correlations between these factors and the subjective grades of corneal staining, given that subjective grading has been used extensively to quantify and monitor corneal staining. The subjective gradings were conducted by 13 trained observers, who were familiar with corneal staining observed by slit lamp, all from the UC Berkeley School of Optometry. The age of the graders was between 24 and 42 years. The graders’ clinical years of experience ranged 2 to 18. A training session was given to the graders to clarify any confusion of using the grading scales and to minimize the variability of using the scales. We provided the graders with standardized descriptions and illustrations of each grading system, which allowed for quantification of the severity of corneal staining. The subjective grading scales used in our study included CCLRU,<sup>5</sup> Efron,<sup>6</sup> and Nation Eye Institute (NEI) scales, which are common grading scales in eye clinics. All grading systems provided

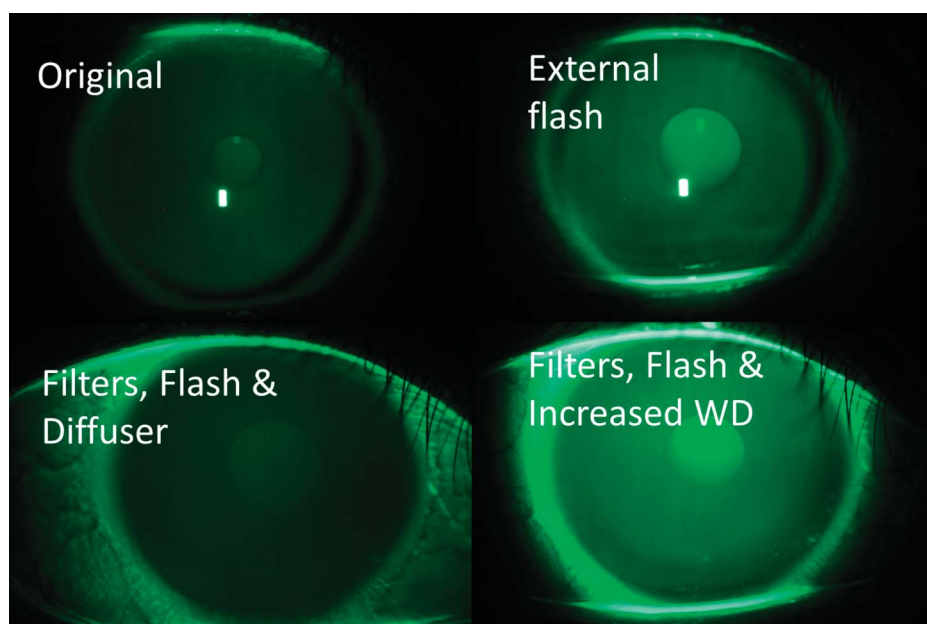
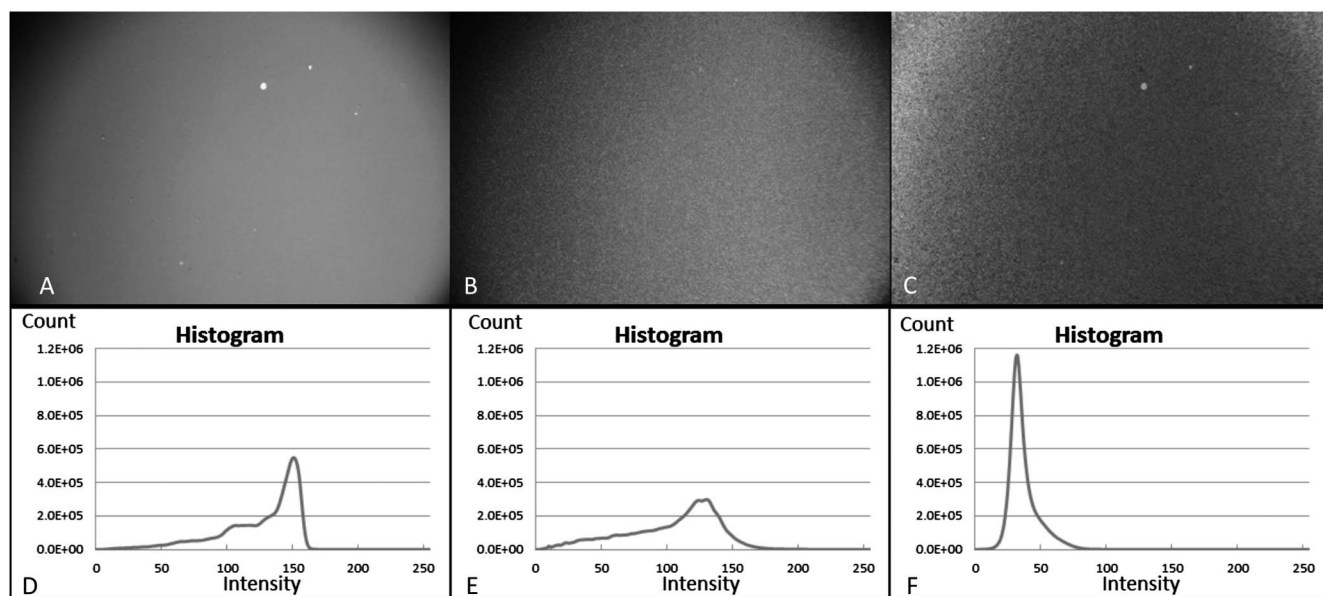


FIG. 2. Step-by-step improvement of the quality of corneal fluorescence image.



**FIG. 3.** “Uniform” illumination after postexperiment processing based on equation 1 by assigning the intensity weight on each pixel. From upper left to lower right are subfigure (a) the original fluorescence image; (b) the illumination distribution image; (c) the intensity-weighted images processed from image (a), and with their corresponding histograms shown in (d), (e), and (f), respectively.

a standardized definition of each grade while Efron and CCLRU scales also included image illustrations. To minimize the interobserver variability, all 13 graders used the same computer with the same monitor (Dell Precision T7500 (Round Rock, TX) with Intel Xeon CPU E5620 (Santa Clara, CA) and ATI FirePro V4800 professional graphics card [Markham, Ontario, Canada]) and display setting (1920 × 1200) in one same room with consistent lighting. The average of the subjective grades on each original image was calculated. A linear ordinary least square regression model was used to measure the relationship between the subjective grades and each of the three objective grades. Such subjective-objective correlations for both the original and the post-processed images with quasi-even illumination were analyzed. Based on the subjective grades, the images we provided to the graders had a wide range of severity of corneal staining. Mean subjective grading scores were 0 to 2.95 for CCLRU (type), 0 to 3.85 for CCLRU (extend), 0 to 2.60 for CCLRU (depth), 0 to 3.10 for Efron, and 0.10 to 2.45 for NEI.

**RESULTS**

An improved corneal fluorescence image was obtained after hardware modifications. Figure 2 illustrates the step-by-step improvement from the modifications, including integrating the

external flash, replacing the filter set, disqualifying the diffuser, and increasing the WD between the slit lamp and the anterior ocular surface. We then conducted a test to validate the proposed image-processing method of adjusting pixel intensity weighted by illumination distribution based on equation 1. The result is shown in Figure 3, where (a), (b), and (c) are the original fluorescence image, the illumination distribution image, and the intensity-weighted images processed from image (a), respectively, with their corresponding histograms shown in Figure 3(d–f). The histogram representing the emission intensity distribution after intensity-weighted processing (Fig. 3f) was the narrowest compared with the histograms of the original fluorescence image (Fig. 3d) and the illumination distribution image (an image of a piece of diffusive paper [Fig. 3e]).

The comparison of the three intensity distributions validated the procedure we used to process the original fluorescence images by using equation 1 to generate new images, which were equivalent to the images captured under a uniform illumination. To record the illumination distribution profile used to calculate the weight of pixel intensity in equation 1, we imaged a white diffusive surface every time after we imaged a subject and then normalized the intensity of each pixel based on the maximum intensity in the image.

**TABLE 1.** Summary of the Correlations of SP (SP-M and SP-A) and SA in Original Images With Five Subjective Grades

	CCLRU (Type)	CCLRU (Depth)	CCLRU (Extent)	Efron	NEI
SP-M	1.36+0.11x R <sup>2</sup> =0.11; P=0.15	1.03+0.09x R <sup>2</sup> =0.13; P=0.12	1.08+0.31x R <sup>2</sup> =0.56; P=0.00	1.29+0.18x R <sup>2</sup> =0.30; P=0.01	1.07+0.11x R <sup>2</sup> =0.24; P=0.03
SP-A	1.40+0.08x R <sup>2</sup> =0.13; P=0.12	1.04+0.07x R <sup>2</sup> =0.18; P=0.07	1.33+0.18x R <sup>2</sup> =0.37; P=0.00	1.43+0.11x R <sup>2</sup> =0.21; P=0.04	1.14+0.07x R <sup>2</sup> =0.20; P=0.05
SA	1.29+0.01x R <sup>2</sup> =0.13; P=0.12	0.94+0.01x R <sup>2</sup> =0.19; P=0.05	0.78+0.04x R <sup>2</sup> =0.81; P=0.00	1.15+0.02x R <sup>2</sup> =0.40; P=0.00	1+0.01x R <sup>2</sup> =0.28; P=0.02

SA, staining area; SP, staining pixel; SP-A, automatically defined threshold; SP-M, manually defined threshold.



**TABLE 2.** Summary of the Correlations of SP (SP-M and SP-A) and SA in Processed Images (Quasi-evenly Illuminated Images) With Five Subjective Grades

	CCLRU (Type)	CCLRU (Depth)	CCLRU (Extent)	Efron	NEI
SP-M	1.24+0.20x $R^2=0.30$ ; $P=0.01$	0.94+0.15x $R^2=0.33$ ; $P=0.01$	1.20+0.32x $R^2=0.47$ ; $P=0.00$	1.25+0.24x $R^2=0.44$ ; $P=0.00$	1.04+0.16x $R^2=0.37$ ; $P=0.00$
SP-A	1.30+0.13x $R^2=0.20$ ; $P=0.05$	0.99+0.10x $R^2=0.23$ ; $P=0.03$	1.11+0.28x $R^2=0.61$ ; $P=0.00$	1.31+0.16x $R^2=0.33$ ; $P=0.01$	1.10+0.10x $R^2=0.25$ ; $P=0.02$
SA	1.47+0.006x $R^2=0.04$ ; $P=0.41$	1.10+0.005x $R^2=0.05$ ; $P=0.33$	1.01+0.03x $R^2=0.68$ ; $P=0.00$	1.35+0.01x $R^2=0.22$ ; $P=0.04$	1.15+0.008x $R^2=0.12$ ; $P=0.13$

SA, staining area; SP, staining pixel; SP-A, automatically defined threshold; SP-M, manually defined threshold.

### Correlation Between Subjective and Objective Grading Systems

A series of linear regression analyses were performed to investigate the correlation between objective grades (of both original and processed images), including SP-M, SP-A, and SA, and subjective grades (of original images only), including CCLRU (type, extent, and depth), Efron, and NEI. Tables 1 and 2 present linear correlations between each pair of objective and subjective grades. All three objective grades, obtained from original images, were significantly correlated with CCLRU (extent), Efron, and NEI grades, whereas correlations between SP-M and CCLRU (type and depth), SP-A and CCLRU (type and depth), and SA and CCLRU (type) were insignificant. After postexperiment processing of the images (to generate quasi-even illumination), SP-M and SP-A showed significant correlations with all subjective grades, and the correlations were stronger. For example, the  $R^2$  of SP-A and CCLRU (extent) increased from 0.37 to 0.61 after quasi-even illumination was applied. We also noted that the correlation between SA and subjected grades was not enhanced. Therefore, quasi-evenly illuminated images improved the predictability of objective grading with SP-M and SP-A. The correlation with CCLRU type and depth became significant after uniformity of illumination was improved.

### Differentiation Capability of Objective Grading System

The objective grading system presented in this study provides a reliable alternative method to the subjective grading system, with its own advantages, for example, enhanced differentiation capability. This capability was revealed in the following experiment. The average subjective grades of staining extent based on the CCLRU scale are same for the two images in Figure 4 (CCLRU [extent]=3.0), although some graders might sense the difference when comparing them side-by-side. However, the objective grading system did yield different grading scores:

SP-M=6.15% and SP-A=10.13% for the left image and SP-M=3.71% and SP-A=5.73% for the right image, indicating a mildly higher staining extent in the left image. Conclusively, objective grading was superior to the subjective grading scale in its capability to quantify minor differences between those two images.

### DISCUSSION

In the present study, we first modified a commercial slit lamp by replacing the original film camera with a new digital camera, upgrading the filter set for fluorescence imaging, and enlarging the WD. In addition to the modification of the hardware, we introduced an additional step for image processing to generate a quasi-even illumination and minimize the artifacts caused by uneven illumination.

With modifications of a commercial slit lamp and postexperiment image-processing technique, we demonstrated that our objective grading system provided an alternative tool to a subjective grading system. The quantification technique of fluorescence presented in this study has its own advantage. The digitization of high-quality fluorescence images can contribute to longitudinal study of anterior ocular health assessment. Also, a computer-aided analysis of a digital image has better differentiation capability than a subjective grading system (e.g., 256 intensity levels in an 8-bit grayscale image vs. 0–4 score [9 levels if in a 0.5 increment]).

However, further improvement is still needed. First, to create quasi-even illumination, a small amount of noise was introduced with manipulation of emission intensity because of texture on the diffusive surface. A smoother but still 100% diffusive surface, working as the “white” background for obtaining illumination intensity distribution, is desired to reduce the noise. Second, uneven distribution of tear film can be misleading when observers search for corneal staining spots. Specifically, the intensity of staining spots in one region may be darker than the background (tear

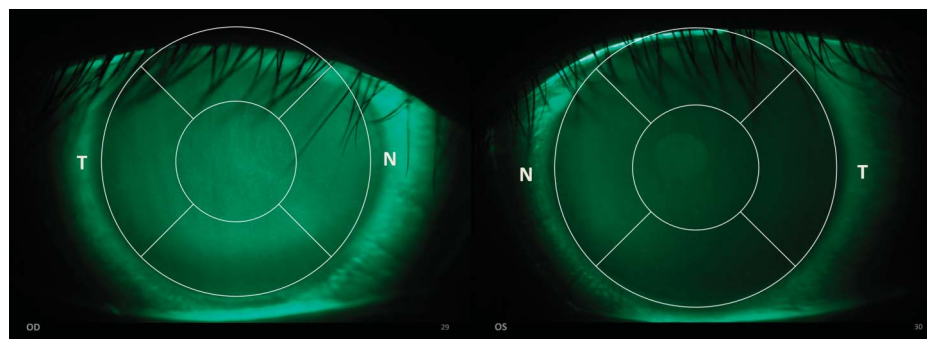


**FIG. 4.** Differentiation capability of objective grading—Extent: CCLRU=3.0 for temporal zone at both images versus (left) SP-M=6.15% and SP-A=10.13% versus (right) SP-M=3.71% and SP-A=5.73%. SP, staining pixel; SP-M, manually defined threshold; SP-A, automatically defined threshold.

film) in another region. Therefore, smaller subzones with relatively consistent background need to be defined and analyzed separately. Third, other objective grades, for example, max, mean, and standard deviation of fluorescence intensity, are worth investigation. For example, when using the standard deviation or intensity gradient, which better represents the dispersion of the stains than the sum of pixels of the region, we might see a higher correlation with CCLRU (depth). Lastly, the fluorescence intensity variation with decreasing concentration of dye can also be used to quantify tear volume, tear mixing, and tear turnover rate with certain types of calibration.

In conclusion, the quality of corneal surface fluorescence images was significantly improved with slit lamp hardware modification and postexperiment image processing. To demonstrate the advantages of the improved imaging technique, objective grading was performed on the improved corneal staining images before and after postexperiment image processing. The statistically significant correlation with the subjective grading system illustrated the reliability of our objective grading technique. The present objective grading of corneal staining is also superior to the subjective grading method in its ability to differentiate small differences of corneal staining. In our future studies, we will investigate potential applications of the present imaging technique to quantify tear retention time on the ocular surface of normal and dry eyes as well as post-contact lens tear mixing.

## REFERENCES

- Morgan PB, Maldonado-Codina C. Corneal staining: Do we really understand what we are seeing? *Cont Lens Anterior Eye* 2009;32:48–54.
- Peterson RC, Wolffsohn JS. Objective grading of the anterior eye. *Optom Vis Sci* 2009;86:273–278.
- Tang K, Le Beck D, Weissman BK. Shooting a film photo slit lamp into the digital age. *Optom Vis Sci* 2006;83:616–618.
- Cox I, Fonn D. Interference filters to eliminate the surface reflex and improve contrast during fluorescein photography. *Int Contact Lens Clin* 1991;18:178–181.
- Phillips AJ, Speedwell L, Makepeace C. CCLRU grading scales (Appendix D). In: *Contact Lenses*. Oxford, United Kingdom, Butterworth-Heinemann, 1997, pp 863–867.
- Efron N. *Contact Lens Complications*. Oxford, UK, Butterworth-Heinemann, 1999.
- Haugland HP. *Handbook of Fluorescent Probes and Research Products*. Eugene, OR, Molecular Probes, 2002, pp 46–47.
- Lin MC, Graham AD, Polse KA, et al. Measurement of post-lens tear thickness. *Invest Ophthalmol Vis Sci* 1999;40:2833–2839.
- Creech JL. *Study of the Aqueous Tear Film and Implications for Contact-Lens Wear*. University of Berkeley, Berkeley, CA. 1998.
- Webber WRS, Jones DP. Continuous fluorophotometric method of measuring tear turnover rate in humans and analysis of factors affecting accuracy. *Med Biol Eng Comput* 1986;24:386–392.
- Mishima S, Gasset A, Klyce SDJ, et al. Determination of tear volume and tear flow. *Invest Ophthalmol* 1966;5:264–276.
- Webber WRS, Jones DP, Wright P. Fluorophotometric measurements of tear turnover rate in normal healthy persons: Evidence for a circadian rhythm. *Eye (Lond)* 1987;1:615–620.
- Puffer MJ, Neault RW, Brubaker RF. Basal precorneal tear turnover in the human eye. *Am J Ophthalmol* 1980;89:369–376.
- Kuppens EVMJ, Stolwijk TR, de Keizer RJW, et al. Basal tear turnover and topical timolol in glaucoma patients and healthy controls by fluorophotometry. *Invest Ophthalmol Vis Sci* 1992;33:3442–3448.
- Occhipinti JR, Mosier MA, Lamotte J, et al. Fluorophotometric measurement of human tear turnover rate. *Curr Eye Res* 1988;7:995–1000.
- Mitsubayashi K, Ogasawara K, Yokoyama K, et al. Measurement of tear electrolyte concentration and turnover rate using a flexible conductimetric sensor. *Technol Health Care* 1995;3:117–121.
- Xu K-P, Tsubota K. Correlation of tear clearance rate and fluorophotometric assessment of tear turnover. *Br J Ophthalmol* 1995;79:1042–1045.

## Appendix 1: MODIFICATIONS OF ILLUMINATION SYSTEM OF NIKON FS-2 SLIT LAMP

### Removing the “Hot Spot” From Corneal Fluorescence Images

To remove the hot spot from the corneal staining image, we first needed to locate the source of this bright spot. The fluorescence image is formed by the emission light from the fluorescein dye excited by blue excitation light. The emission light has a longer wavelength than the excitation light, hence lower energy than the absorbed radiation. Sodium fluorescein has excitation and emission spectrum peaks of approximately 495 nm and 521 nm, respectively.<sup>7</sup> Nikon FS-2 was originally equipped with cobalt blue and yellow filters to enhance fluorescence image quality by separating excitation and emission lights. However, excitation and emission lights have an overlap in their spectra at approximately 500 nm. The blue and yellow filters used in most conventional slit lamps also have an overlap of the wavelength passbands. Therefore, in the original slit lamp setup, a yellow filter could not completely block the excitation beams reflected off the curved cornea surface, which resulted in a portion of reflection leaking into the imaging path and forming a saturated reflection spot on the cornea fluorescence images because of curvature of cornea. To correct for this overlap in wavelengths, we replaced the original filters with a new filter set, band-pass filter “ET470/40X” and long-pass filter “HQ510LP,” originally made for epifluorescence microscopes, which could separate the excitation and the emission light because of the separation of band pass, as shown in Figure 5.

### Expanding the Illumination Area

To generate a larger illumination zone covering the entire cornea (i.e., limbus to limbus), we initially tried a diffuser. The illumination did cover the whole anterior ocular surface with the diffuser in front of the eye, but the illumination intensity dropped significantly. The reduction of intensity made it difficult to preview and focus the camera unless we increased ISO of the camera, which would in turn lead to increased imaging noise. An alternate solution was to expand the illumination area by increasing the WD, that is, moving the slit lamp farther away from the cornea. Thus, the image distance (the distance between the focusing lens and camera) should be shortened to maintain the best focus of the cornea on the camera image surface. We therefore moved the lens mount toward the camera. Figure 5 illustrates the modification.

## Appendix 2: POSTEXPERIMENT IMAGE PROCESSING TO GENERATE QUASI-EVEN ILLUMINATION

To investigate the question of how the distribution of the illumination could be “transformed” into quasi-even coverage so that a single photo could provide an overview of the true condition of the cornea, we first examined the correlation between the intensity distribution of excitation and emission lights.

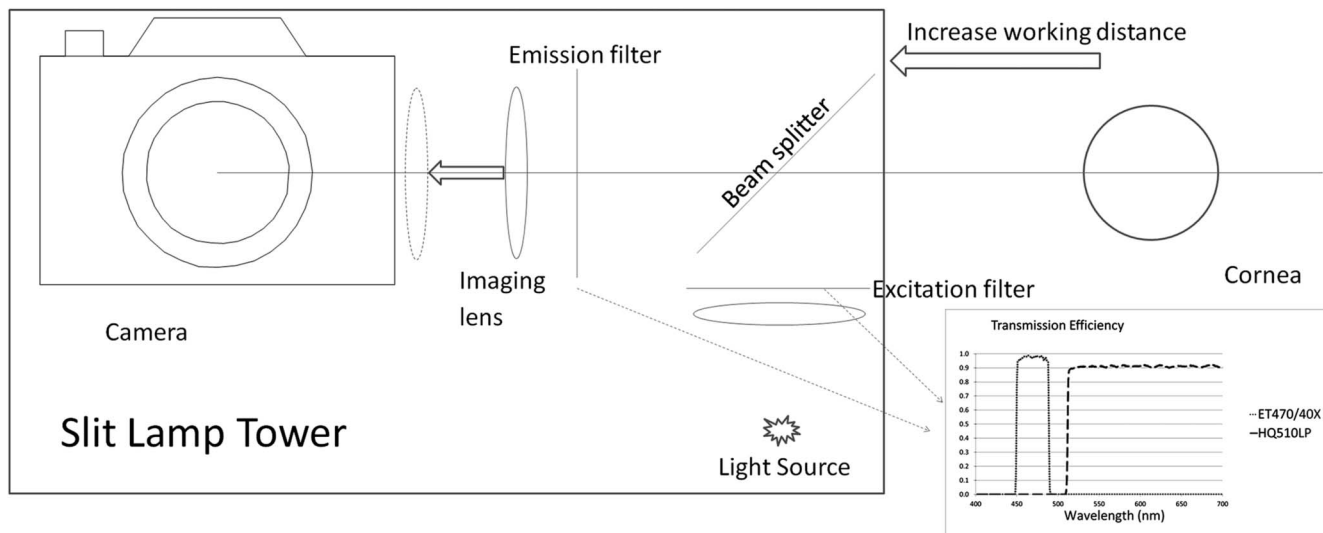


FIG. 5. Diagram of modified FS-2 slit lamp, including the increased working distance enlarged the area illuminated by the light source on the cornea transmission efficiency of the new excitation (ET470/40X) and emission (HQ510LP) filters (generated from the specifications provided on www.chroma.com).

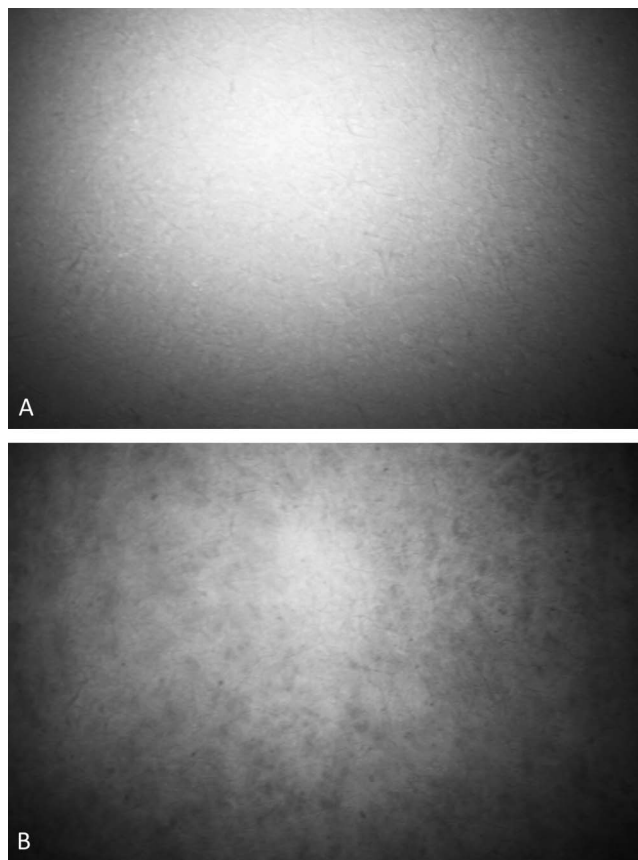


FIG. 6. “Green” images extracted from RGB photos of a white 100% diffusive paper (A) and a black sodium fluorescein-soaked paper (B). The slit lamp and the camera had the same setting except for adding the blue filter when imaging the black paper.

We imaged two pieces of paper, a white paper with the characteristics of nearly 100% diffusive reflection and a black paper soaked with sodium fluorescein solution. Green light was used as illumination to image the white paper, whereas blue light (white light through ET470/40X filter) was used to illuminate the sodium fluorescein-soaked black paper. We extracted the green color from the original RGB photos (Fig. 6). Then, linear regression was performed on the intensity of each two corresponding pixels in the two photos. The regression result confirmed a significant and strong linear correlation between the illumination (excitation) and fluorescence (emission) intensity ( $R^2=0.9638$ ,  $P=0.000$ ). The correlation regression coefficients are shown in Table 3. A mathematical model (equation 1) was then built to transform the pixel intensity in the original fluorescence image by applying a “weight” that was determined by the normalized intensity of each pixel. The post-processed image with transformed pixel intensity is equivalent to an image under quasi-even illumination.

### Appendix 3: DETERMINATION OF INITIAL CONCENTRATION AND VOLUME OF SODIUM FLUORESCIN

#### Quenching Effect

We developed a test to find the optimal fluorescein concentration to get the maximum fluorescence intensity in linear regime. Figure 7 shows an investigation of the correlation relationship between fluorescence intensity and fluorescein concentration. We found that the fluorescein concentration corresponding to

TABLE 3. Linear Correlation Between Excitation and Emission Intensity

Emission intensity	Coefficient	Standard Error	P	95% Confidence Interval
Excitation intensity	0.856	0.00004	0.000	0.855974–0.8561276



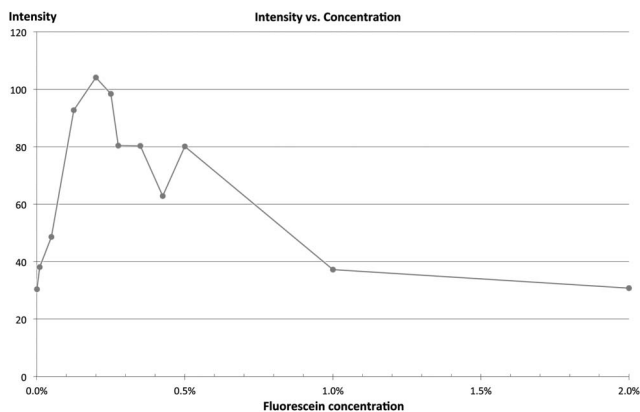


FIG. 7. Demonstration of quenching effect in a tear film model (fluorescein solution sandwiched by two coverslips); the concentration showing optimal fluorescence is 0.2%.

the maximum fluorescence intensity was approximately 0.2% for a 10- $\mu$ m layer of sodium fluorescein solution, which has similar dimension as pre-lens and post-lens tear film.<sup>8,9</sup> This result is consistent with the finding by another study, although in that study a fluorometer was used to monitor and record emission intensity.<sup>10</sup>

To maintain the optimal fluorescein concentration (0.2%) producing high fluorescence intensity, the initial concentration and volume of dye solution instilled onto the eye, tear volume, tear turnover rate, and the elapsed time between dye instillation and

observation (snapshot) had to be considered. The postulated average values of these factors were obtained from previously published literature: average tear turnover rate is between 11% and 44% per minute<sup>10-16</sup>; average tear volume is between 6.2 and 9.7  $\mu$ L<sup>11,17</sup>; and the concentration of fluorescein in the eye at time ( $t$ ) after the instillation is given by<sup>11</sup>

$$C_t = C_0 \exp(-kt), \tag{4}$$

where  $C_0$  is the initial concentration and  $k$  is the turnover rate. Therefore, we can derive an equation to calculate the initial concentration of fluorescein sodium solution instilled into the eye. This initial concentration of fluorescein sodium in eyes could guarantee the capture of optimal fluorescence after 60 to 70 sec, the time needed to align and focus the slit lamp and for the fluorescein sodium to dilute evenly in human tears. The equation is

$$C_0 = C_t \exp(kt). \tag{5}$$

Therefore, assuming the lowest initial concentration (the max tear volume 9.7  $\mu$ L) after instillation and the fastest turnover rate (44% per minute),  $C_0$  should be 0.33%. We determined that 2  $\mu$ L 2% sodium fluorescein solution should be instilled into the eye to capture the optimal fluorescence (at the concentration of  $\sim$ 0.2%). It should be noted that the tear volume and tear turnover rate vary from one subject to another, so we took multiple images after 60 sec until fluorescence intensity began to decrease, thereby accounting for individual patient variations to capture optimal fluorescence intensity.